Submitted to Geophysics

LBL-7032
Preprint



# MAGNETOTELLURICS WITH A REMOTE MAGNETIC REFERENCE

Thomas D. Gamble, Wolfgang M. Goubau, and
John Clarke

January 1978

Prepared for the U. S. Department of Energy
under Contract W-7405-ENG-48



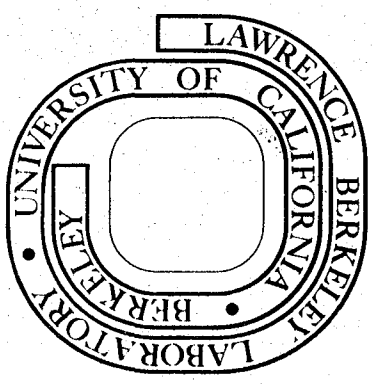

Submitted to Geophys.

# MAGNETOTELLURICS WITH A REMOTE MAGNETIC REFERENCE

THOMAS D. GAMBLE*, WOLFGANG M. GOUBAU*, AND JOHN CLARKE*

## ABSTRACT

Magnetotelluric measurements were performed simultaneously at two sites 4.8 km apart near Hollister, California. SQUID magnetometers were used to measure fluctuations in two orthogonal horizontal components of the magnetic field. The data obtained at each site were analyzed using the magnetic fields at the other site as a remote reference. In this technique, one multiplies the equations relating the Fourier components of the electric and magnetic fields by a component of magnetic field from the remote reference. By averaging the various crossproducts, one can obtain estimates of the impedance tensor that are unbiased by noise, provided there are no correlations between the noises in the remote channels and the noises in the local channels. Even for data for which the E-E predicted coherencies were as low as 0.1, the apparent resistivities obtained from this technique were consistent with apparent resistivities calculated from high coherency data at adjacent periods. Apparent resistivities calculated by conventional analysis of the same data were biased by as much as two orders of magnitude. The estimated standard deviation for periods shorter than 3 s was less than 5%, and,

* Department of Physics, University of California, and Materials and Molecular Research and Earth Sciences Divisions, Lawrence Berkeley Laboratory, Berkeley, California 94720.

for 87% of the data, was less than 2%. Where data bands overlapped between periods of 0.33 s and 1 s, the average discrepancy between the apparent resistivities was 1.8%.

## INTRODUCTION

In the magnetotelluric (MT) method, one seeks the elements of the impedance tensor $\underline{\underline{Z}}(\omega)$ from the equations

$$E_x(\omega) = Z_{xx}(\omega)\, H_x(\omega) + Z_{xy}(\omega)\, H_y(\omega) \ , \tag{1}$$

and

$$E_y(\omega) = Z_{yx}(\omega)\, H_x(\omega) + Z_{yy}(\omega)\, H_y(\omega) \ . \tag{2}$$

In equations (1) and (2), $H_x(\omega)$, $H_y(\omega)$, $E_x(\omega)$, and $E_y(\omega)$ are the Fourier transforms of the fluctuating horizontal magnetic and electric fields $H_x(t)$, $H_y(t)$, $E_x(t)$, and $E_y(t)$. If one multiplies equations (1) and (2) in turn by the complex conjugate of each of the frequency-dependent fields and averages the resulting autopowers and crosspowers of the fields over many sets of data, one obtains eight simultaneous equations that can be solved for the impedance elements. As is well known, the autopowers may severely bias the impedance estimates if there is noise in the measured fields (Sims, Bostick, and Smith, 1971, and Kao and Rankin, 1977). In an earlier paper (Goubau, Gamble, and Clarke, 1978) we discussed two different approaches to reducing this bias: A solution of the eight simultaneous equations for the impedance elements in terms of crosspowers alone, and a solution of the equations in terms of weighted crosspowers. We also discussed analysis techniques for MT measurements with a fifth (electric or magnetic) local reference channel, including a crosspower analysis in which one multiplies equations (1) and (2) by the complex conjugate of the Fourier transform of the reference field. We concluded that any of the 4- or 5-channel methods would work satisfactorily provided that the noise in the various channels was uncorrelated. We tested several

of these techniques on data obtained at Grass Valley, Nevada. In most of our measurements, we found that there was a significant level of correlated noise between at least some channels, and that most of our techniques yielded apparent resistivities that were biased.

Finally, we proposed the use of a remote magnetometer to obtain reference fields $H_{xr}(t)$ and $H_{yr}(t)$ in which the noise should be uncorrelated with any of the four fields at the MT station. One solves equations (1) and (2) by multiplying them in turn by $H^*_{xr}(\omega)$ and $H^*_{yr}(\omega)$ to obtain four equations that can be solved for the impedance elements. One finds:

$$Z_{xx} = (\overline{E_x H^*_{xr}}\ \overline{H_y H^*_{yr}} - \overline{E_x H^*_{yr}}\ \overline{H_y H^*_{xr}})/D \ , \tag{3}$$

$$Z_{xy} = (\overline{E_x H^*_{yr}}\ \overline{H_x H^*_{xr}} - \overline{E_x H^*_{xr}}\ \overline{H_x H^*_{yr}})/D \ , \tag{4}$$

$$Z_{yx} = (\overline{E_y H^*_{xr}}\ \overline{H_y H^*_{yr}} - \overline{E_y H^*_{yr}}\ \overline{H_y H^*_{xr}})/D \ , \tag{5}$$

and

$$Z_{yy} = (\overline{E_y H^*_{yr}}\ \overline{H_x H^*_{xr}} - \overline{E_y H^*_{xr}}\ \overline{H_x H^*_{yr}})/D \ , \tag{6}$$

where $D \equiv \overline{H_x H^*_{xr}}\ \overline{H_y H^*_{yr}} - \overline{H_x H^*_{yr}}\ \overline{H_y H^*_{xr}}$ .

The bar denotes an average over all transform points within a given frequency window, and over all sets of data. The impedance elements will be unbiased by noise provided the noise in the MT array is uncorrelated with noise in the reference channels. It should be noted that since each of equations (1) and (2) is multiplied in turn by a single reference field, the values of the impedance elements are independent of the magnitudes and phases of the reference fields. Therefore, one does not need a precise knowledge of the gains or phase shifts in the telemetry for the remote references.

In this paper, we describe a test of the remote reference technique in Bear Valley, near Hollister, California, where we set up two magnetotelluric stations, and simultaneously recorded $E_x$, $E_y$, $H_x$, $H_y$, and $H_z$ from both stations. The standard analysis techniques yielded apparent resistivities that were significantly biased by noise. However, the use of the remote reference enabled us to obtain apparent resistivities that had no obvious bias even when the coherencies were as low as 0.1. Furthermore, where the highest frequency band and second highest frequency band overlapped, the apparent resistivities agreed to within 1.8%. The estimated standard deviation for the apparent resistivities at periods shorter than 3 s was 1.3%.

## MEASUREMENTS

We established two complete MT stations separated by 4.8 km on La Gloria road in Bear Valley, California, at the sites shown in Figure 1. The Upper La Gloria station is in hilly terrain where the geology consists chiefly of granites, while the Lower La Gloria station is in a level area over a zone of low resistivity (Mazella, 1965), and is slightly east of a fault that separates this zone from the granites. Lower La Gloria is about 2 km west of the San Andreas Rift Zone.

For the electric field measurements we used the Pb electrodes installed by Corwin for dipole-dipole resistivity monitoring (Morrison, Corwin, and Chang, 1977). The location of the electrodes is shown in Figure 1. Electrodes $E_1$ and $E_2$ were the common electrodes at the lower and upper

stations, respectively. In the subsequent analysis we made the electric field directions at each station orthogonal. For the magnetic field measurements we used our dc SQUID 3-axis magnetometer (Clarke, Goubau, and Ketchen, 1976) at Lower La Gloria, and an rf SQUID 3-axis magnetometer manufactured by S.H.E. Corporation at Upper La Gloria. The magnetic field sensitivities were approximately $10^{-5}\,\gamma\,Hz^{-\frac{1}{2}}$ and $10^{-4}\,\gamma\,Hz^{-\frac{1}{2}}$, respectively. The magnetometer at each site was used as the reference for the MT signals at the other site.

We recorded simultaneously the MT data and the vertical components of the magnetic field fluctuations at each site. A block diagram of the measurement electronics appears in Figure 2. The equipment at Lower La Gloria was battery powered, while that at Upper La Gloria was powered by a 60 Hz generator. Each signal was passed through a preamplifier that contained a high-pass filter to attenuate the large-amplitude low-frequency signals that could have exceeded the dynamic range of the electronics. Each preamplifier was followed by a 60-Hz notch filter. The signals from Lower La Gloria were transmitted to Upper La Gloria by FM telemetry via a repeater on Willow Creek Peak. At Upper La Gloria we passed each of the eight MT signals and two vertical components of magnetic field through a four-pole band-pass filter, digitized the signals with 12-bit resolution, and recorded the data on a nine-track digital recorder. Data acquired in the four overlapping bands are listed in Table 1. Band 4 was intended to include periods from 30 s to 1000 s, but an error in setting the high-pass filter of the telemetry preamplifier at the remote site resulted in the longest period being 100 s. The times required for data collection and the sampling periods are also listed in Table 1. We recorded all the

data within a 40-hour period, making only brief interruptions to change gains and filter bands and to replace batteries.

## DATA PROCESSING

Using the CDC 7600 computer facility of the Lawrence Berkeley Laboratory, we processed our data, graphed it on microfilm, and visually inspected the records. Rejecting data that had been rendered meaningless by equipment failure, amplifier saturation, or magnetic interference from passing vehicles, we then arranged the remaining data into segments containing the number of points shown in Table 1. We subtracted the mean value and linear trend from each segment, multiplied the ends of the segments by a cosine bell window, and computed the fast Fourier transform. The necessary crosspower and autopower densities were calculated by multiplying the Fourier coefficients for the various fields together, and averaging the products over all of the data segments and over the Fourier harmonics contained in non-overlapping frequency windows of $Q = 3$. The center period of each window, the number of harmonics in each window, and the number of segments are given in Table 2.

## DATA ANALYSIS

We computed impedance tensors for both MT stations as a function of period using equations (3) to (6). For comparison we also computed the impedance tensors using the following three methods: (1) We found the impedance tensor that minimized the mean square of $|\vec{E} - \underline{\underline{Z}}\,\vec{H}|$. We refer to this method as the standard analysis since it is the method that is most commonly used (Vozoff, 1972). Impedances calculated by this method depend on autopowers of the magnetic fields. As a result, the magnitudes of the impedance tensor elements are biased downward by the noise power in the magnetic channels. (2) We computed $\underline{\underline{Z}}$ from the inverse of the admittance tensor $\underline{\underline{Y}}$, where $\underline{\underline{Y}}$ was chosen to minimize the mean square of $|\vec{H} - \underline{\underline{Y}}\,\vec{E}|$. We refer to this calculation as the admittance method which biases the magnitudes of the impedance tensor elements upward by the noise power in the electric fields (Sims, Bostick, and Smith, 1971). (3) We computed $\underline{\underline{Z}}$ in terms of crosspowers of the four fields measured at each station. As we have shown (Goubau, Gamble, and Clarke, 1978) there is sufficient information in the crosspower data to enable one to obtain estimates of $\underline{\underline{Z}}$ that are not biased by the noise power in any of the channels. We refer to this analysis as the crosspower method.

For each method of analysis we rotated the coordinate axes to maximize $|Z_{xy}|^2 + |Z_{yx}|^2$, thereby aligning one of the axes parallel to the strike direction, if such a direction existed. We then computed the off-diagonal elements, $\rho_{xy}$ and $\rho_{yx}$, of the rotated apparent resistivity tensor from the expressions

$$\rho_{xy} = 0.2 \, |Z_{xy}|^2 \, T \, , \tag{7}$$

$$\text{and} \quad \rho_{yx} = 0.2 \, |Z_{yx}|^2 \, T \, , \tag{8}$$

where $\rho_{xy}$ and $\rho_{yy}$ are in $\Omega$m, T is the period in seconds, and $Z_{xy}$ and $Z_{yx}$ are in units of (mV/km) $\gamma^{-1}$. For the standard and remote reference analyses we also calculated the phases of $Z_{xy}$ and $Z_{yx}$ and the skewnesses, $|(Z_{xx} + Z_{yy})/(Z_{yx} - Z_{xy})|$.

To obtain an estimate of the noise in our data, we computed the coherency between the measured electric field $\vec{E}$ and the electric field $\vec{E}_p$ predicted from $\vec{E}_p = \underline{\underline{Z}} \, \vec{H}$, where $\underline{\underline{Z}}$ was obtained from the standard analysis. The coherencies are defined by $C_i = \overline{E_i E_{ip}^*} \left( \overline{|E_i|^2} \, \overline{|E_{ip}|^2} \right)^{-\frac{1}{2}}$, where i = x, y. For the standard analysis one can show that $\overline{E_i E_{ip}^*} \equiv \overline{|E_{ip}|^2}$, so that

$$C_i = \left( \overline{|E_{ip}|^2} \Big/ \overline{|E_i|^2} \right)^{\frac{1}{2}} \quad (i = x, y) \, . \tag{9}$$

## GRAPHICAL COMPARISON OF APPARENT RESISTIVITIES

The results for Upper La Gloria are summarized in Figures 3 to 9, and for Lower La Gloria in Figures 10 to 16. Figures 3 through 6 show the apparent resistivities as a function of period for the standard, admittance, crosspower, and remote reference methods at the Upper La Gloria station.* The apparent resistivities from the remote reference method are repeated as dashed lines on Figures 3 and 5 to facilitate comparison with the other methods. The coherencies $C_x$ and $C_y$ are plotted in Figure 7.

*The windows at 0.023 s and 0.325 s contain harmonics outside the bandpass of the filters, and would ordinarily not be used. However, we plotted

(cont'd)

Comparing Figures 3 and 4, we see that both the standard and admittance methods yield resistivities that vary smoothly over wide ranges of periods. However, both methods yield discontinuities in $\rho_{xy}$ where bands overlap at periods of 3 and 30 s. We will discuss these discontinuities later and show that they are not caused by systematic errors in data processing. The standard analysis also shows a large dip in $\rho_{yx}$ at 0.03 s that does not appear in the admittance results, and that is not associated with any anomaly in $C_y$ (Figure 7). We believe that this dip is caused by the magnetic noise from the generator at the Upper La Gloria station.

Although the apparent resistivity curves from the standard and admittance methods are fairly smooth, there are significant systematic discrepancies. The resistivities from the admittance analysis are higher than those from the standard analysis in all cases except four on the y-axis near 40 s period. By comparing Figures 3 and 4 with Figure 7 we see that the discrepancies generally increase as the coherency $C_i$ decreases. The best agreement between the two methods is for periods shorter than 2 s. For periods shorter than 3 s, $C_x$ is greater than 0.9, and most values of $\rho_{xy}$ in Figure 4 are about 10% higher than those in Figure 3, although the disagreement does increase to a factor of 2 at 3 s period. For C between 0.9 and 0.6 the disagreement is

---

the apparent resistivities from the 0.023 s window to demonstrate the narrow band nature of the noise in the 0.032 s window. The apparent resistivities from the 0.325 s window were used only to interpolate a value of the resistivity to be compared with the result at 0.41 s from band 1.

usually about a factor of two (for example, $\rho_{yx}$ between 0.06 and 1 s periods) but can be much larger (for example $\rho_{yx}$ at 0.032 and 9 s periods). We attribute the systematic differences to the bias errors mentioned earlier.

If we look at the apparent resistivities from the crosspower method, we see that the curves are far more irregular than those from the admittance or standard methods. The random errors of the crosspower analysis depend in a complex way on the value of the impedance tensor, the orientation of the measurement axes, and the relative levels of the noises. However, we believe that the random errors are relatively large primarily because this estimate of the impedance tensor depends strongly on the crosspowers between fields that may be only slightly coherent, such as $\overline{E_x E_y^*}$ (Goubau, Gamble, and Clarke, 1978). The best results from this method are for $\rho_{xy}$ at periods shorter than 1 s, where $C_x$ is greater than 0.9. Here, the resistivities from the crosspower method are still scattered over the 10% range of the disagreement between the standard and admittance resistivities. Note that no value of apparent resistivity has been plotted at 0.032 s period for the crosspower method (Figure 5). This is because this method did not predict real values for the autopowers. Thus we know that there is some significant noise in this window even though $C_y$ is higher than in the adjacent windows (Figure 7).

Because of the large random errors in the crosspower analysis and the bias errors in the two least-squares analyses, we cannot use these methods to obtain reliable estimates of the apparent resistivity when the $C_i$ are less than 0.9. If we were to reject all resistivities for

which $C_i$ is below 0.9, we could retain only 11 values for $\rho_{yx}$, all at periods longer than 0.5 s.

In Figure 6 we see that the apparent resistivities from the remote reference method lie on smoother curves than those from any of the previous methods. Furthermore, the discontinuities and disagreements where bands overlap in Figures 3 and 4 have essentially been eliminated, suggesting that the disagreements were caused by bias errors. In the next section, we quantitatively compare the results from different bands where the bands overlap. At periods where the $C_i$ are high, the remote reference usually agrees well with the standard and admittance methods. For $\rho_{xy}$ between 0.032 and 2 s the apparent resistivities obtained using the remote reference lie about half-way between and are within about 5% of those obtained with the standard and admittance methods.

We produced 64 apparent resistivities from each method of analysis at Upper La Gloria. In 60 cases the apparent resistivities from the admittance method are larger, and those from the standard method are smaller than those from the remote reference method. This regular ordering of the apparent resistivities demonstrates that the bias error in at least two of the methods is large compared to the random error in any of them and it strongly suggests that the bias is due to the use of autopower estimates in the least-squares methods.

The apparent resistivities at Lower La Gloria from the standard, admittance, crosspower, and remote reference methods are shown in Figures 10-13, and the E-E predicted coherencies are shown in Figure 14. Again, the dashed lines in Figures 10 to 12 reproduce the remote reference apparent resistivities from Figure 13. At Lower La Gloria we had more noise than at the upper station. $C_x$ and

$C_y$ are both above 0.9 for only four windows. $C_x$ and $C_y$ are both below 0.5 for periods between 5 and 10 s. At all periods, the apparent resistivities from the admittance method (Figure 11) are higher than the corresponding apparent resistivities from the standard analysis (Figure 10). Thus, as at Upper La Gloria, the bias errors of the least-squares methods are large compared to the random errors. When $C_i$ is lowest, the relative bias is largest. At a period of 9 s the relative bias is about a factor of 20 for $\rho_{yx}$, and about a factor of 100 for $\rho_{xy}$. The peaks and dips in the apparent resistivity curves in Figures 10 and 11 are also so steep that we can be sure that neither least-squares method accurately estimates the apparent resistivity of the ground.

The apparent resistivities from the crosspower analysis at Lower La Gloria (Figure 12) seem to be more stable than they were at Upper La Gloria. For periods shorter than 20 s the crosspower method yields apparent resistivities that lie between the two least squares resistivities in 50 of 54 cases. This result indicates that the random errors for the crosspower method are small in this case compared to the bias errors of the least squares methods, and is further evidence that the autopower bias is the major source of error. At periods between 3 and 20 s, the crosspower analysis yields dips in the apparent resistivity similar to those of the standard analysis, but about a factor of five smaller. We believe that such dips are caused by correlations in the noises, which bias the estimates of the apparent resistivity.

In contrast with the other methods, the remote reference method yields apparent resistivities (Figure 13) that vary smoothly over the entire range of periods, even where the coherency is low. There is

almost no disagreement between overlapping bands. At periods shorter than 1 s, the remote reference apparent resistivities agree with the results from the crosspower method to within the random scatter of the crosspower results (± 10%). The resistivities from the standard method are biased downward by about 10% near 1 s period, and by more than a factor of 2 at the shortest periods.

## QUANTITATIVE EVALUATION OF APPARENT RESISTIVITIES OBTAINED USING REMOTE REFERENCE

In this section we present a more quantitative analysis of the expected errors associated with the apparent resistivities obtained using the remote reference technique. We compute an average disagreement for the apparent resistivities at periods where bands overlap, and obtain a measure of the rms random fluctuations for the resistivities within a single band.

At both Upper and Lower La Gloria there are three values of $\rho_{xy}$ and three values of $\rho_{yx}$ in band 1 at periods that are also contained in band 2. We compared these resistivities with the linear interpolation of the values of apparent resistivity in band 2. We computed the fractional discrepancy between the overlapping resistivities, and averaged the magnitude of this discrepancy over each of the three periods, for both axes and for both stations, to produce the "mean discrepancy" for the 12 resistivities in the region of band overlap. In the same way, we calculated the mean

discrepancy between the overlaps of bands 2 and 3, and bands 3 and 4. The mean discrepancies and the number of resistivities used to obtain each mean discrepancy are shown in Table 3 for both the standard and remote reference analyses.

From Table 3 we see that the mean discrepancies for the remote reference are consistently smaller than those for the standard analysis. The smallest discrepancy is 1.8% between bands 1 and 2. This discrepancy is somewhat smaller than the ± 2% uncertainty in apparent resistivity that we expected because of a ± 1% uncertainty in amplifier gains. Between bands 2 and 3 and bands 3 and 4, the mean discrepancies are larger, but they are still on the order of the random scatter that one sees within a single band by comparing apparent resistivities at adjacent periods. From the good agreement where the bands overlap, we conclude that there are no significant errors associated with the spectral resolution of the Fourier transform. As we see from Table 1, in band 2 we used segments that were 10 times longer than those of band 1. Thus, the spectral resolution of the harmonics in band 2 was ten times higher than the resolution in band 1, and the spectral overlap from narrow peaks in the autopower spectra of the various fields was ten times smaller.

We now estimate the rms errors associated with apparent resistivities within a single band. In Figures 6 and 13 (remote reference analysis) there is no visible scatter between resistivities at adjacent periods for periods shorter than 3 s (i.e. bands 1 and 2). To estimate the random errors in this range we recomputed apparent resistivities for each period, using a smaller number of data segments in the determination

of the average crosspower densities. We sorted our original data segments into N smaller blocks, thereby obtaining N completely independent estimates for the apparent resistivity at each period. We computed the average of the N values, $\bar{\rho}_j$ (j = xy, yx), and the expected deviation of the mean, defined by

$$\rho_j = \left[ \sum_{i=1}^{N} (\rho_{ij} - \bar{\rho}_j)^2 / N(N-1) \right]^{1/2} . \qquad (10)$$

For band 1 at Upper La Gloria we used N = 5 blocks, while for band 1 at Lower La Gloria and for band 2 at both stations we used N = 4 blocks. In an attempt to include signals of various polarizations in each of the N blocks of data segments, we selected for each block roughly equal numbers of records from two different recording times that were widely separated. Table 4 summarizes the recording times and the number of the block to which the data segments were assigned. There are no entries for the first two recording times in band 1 at Lower La Gloria because we had accidentally removed a set of preamplifiers from some of the channels at that station.

Table 5 lists the percentage expected deviation of the mean resistivity, $100\ \rho_j/\bar{\rho}_j$, as a function of period for both stations. We see that the expected fractional deviation of both $\bar{\rho}_{xy}$ and $\bar{\rho}_{yx}$ is always less than 5%, and, for 87% of the data, is 2% or less. The average of $\rho_j/\bar{\rho}_j$ over all entries in Table 5 is 1.3%. For comparison, when we performed the same analysis on the apparent resistivities calculated by the standard analysis, the average of the fractional standard deviation was 3.3%. At periods less than 3 s, the expected deviations are much smaller than the discrepancies caused by bias (typically 20%) that one observes when one

compares these results with those obtained using the remote reference analysis.

## ORIENTATION ANGLES, PHASES, AND SKEWNESSES

We now examine the graphs of the other parameters that may be used in modeling the resistivity of the earth. For Upper La Gloria, Figures 8 and 9 show the orientation angles, $\theta_x$, between the rotated x-axes and magnetic north, the phases of $Z_{xy}$ and $Z_{yx}$, and the skewness as a function of period for the standard and remote reference analyses. We use a right-handed coordinate system with the z-axis pointing down, and the complex phase is $-i\omega t$. The corresponding results for Lower La Gloria are shown in Figures 15 and 16. From Figures 8 and 9 we see that at Upper La Gloria both methods of analysis give physically reasonable values for the orientation angle, phases, and skewness. There is a maximum scatter of about $\pm$ 10° in the phases and $\pm$ 5° in the orientation angle for both methods at periods near 10 s. For both methods, the phase angles where bands 3 and 4 overlap differ by about 5°. However, at periods shorter than 0.1 s the standard analysis yields a scatter of about $\pm$ 3° in orientation angle whereas the remote reference yields no visible scatter. At Lower La Gloria the standard and remote reference methods yield very similar values for the phase angles, with scatter increasing with period up to about $\pm$ 5° for periods longer than 10 s (Figures 15 and 16). The standard analysis yields values of orientation angle and skewness that differ by 20° and 0.2 respectively between bands 2 and 3, while no disagreements are apparent

for the remote reference method. There are also consistent differences between the two methods. For example, the orientation angle at short periods determined by the remote reference method is about 52°, while by the standard method it is about 65°.

## SUMMARY AND DISCUSSION

We have demonstrated the technical feasibility of performing MT soundings using a remote magnetometer as a reference, and we have shown that the results from this method are substantially better than those obtained using the conventional MT technique. We obtained smooth curves of apparent resistivities, orientation angles, phases, and skewnesses as functions of period for both of our stations, even at periods where the coherencies determined from the standard analysis were as low as 0.1. In bands 1 and 2 (periods $< 3$ s) we obtained an estimate of 1.3% for the mean percentage error associated with random variations in the apparent resistivities. At periods where bands 1 and 2 overlapped, the resistivities obtained for the two bands agreed to within an average percentage uncertainty of 1.8%.

By comparing apparent resistivities from the remote reference analysis with apparent resistivities from the standard impedance and admittance analyses, we demonstrated the significance of the bias errors in these least squares methods, and we showed that, in general, there is bias from noise in both electric and magnetic channels. In bands 1 and 2,

where the coherency was between 0.7 and 0.9, the dominant bias was from noise in the magnetic channels, and was typically of the order of 20%. At Lower La Gloria, where the coherencies were as low as 0.1, the standard analysis apparent resistivities at periods near 10 s were biased downward by more than two orders of magnitude, while the apparent resistivities from the admittance method were biased upward by one order of magnitude. We found that the apparent resistivities for the cross-power analysis (which is unbiased by autopower noise) had random errors that often exceeded the bias errors of the two least squares methods.

The results for the remote reference analysis are unbiased by noise in autopowers and by noises that are not correlated over the distance separating the reference magnetometer and the base station. We cannot entirely rule out the possibility of systematic errors caused by long range correlations in the noises, but we feel that the use of the remote reference greatly reduces the likelihood of such systematic errors.

As an alternative to a remote magnetic reference, one could consider using a remote telluric array. However, there are two reasons why we believe telluric arrays may prove to be less reliable as a reference than a magnetic field reference. First, it has been our experience that there is often more noise in the electric measurements than in the magnetic, although this was not the case at the La Gloria stations. Second, the electric field at the surface of the earth produced by a given magnetic field is highly dependent on the geology. The reference must be able to respond in different directions as the polarization of the incident magnetic field changes. If the apparent resistivity is highly anisotropic,

the electric field response tends to lie in the direction of the highest apparent resistivity, and a higher level of random error is produced by a given level of random noise.

The use of a remote magnetic reference should enable one to carry out a magnetotelluric survey in an area contaminated by cultural magnetic and electric noises, provided that the reference is sufficiently far away to ensure that any possible bias errors due to correlated noises are small compared with the random errors. Clearly, the minimum separation depends on both the correlation lengths of the noises and on the length of time over which the data are averaged. The upper limit on the separation is set not only by practical problems of telemetry but also by the coherence length of incoming magnetic signals. When the separation becomes greater than the coherence length, the random errors will increase.

We note that the use of a remote reference may enable one to test the validity of the assumptions usually made in magnetotellurics; for example, that the incident fields are plane waves, and that the electric fields are adequately determined by measurements of the potential difference between widely separated electrodes. The plane wave approximation could be tested by measuring the apparent resistivities as a function of time in an auroral zone (where source effects are likely to be largest) over ground where the true resistivity is believed to be constant. One could examine the effects of electrode placement on the apparent resistivity by measuring apparent resistivities as a function of electrode position. Furthermore, the remote reference technique should allow one to monitor long term changes in the apparent resistivity at a given site to greater accuracy than has previously been possible.

Finally, we feel that the additional cost of the second magnetotelluric station is easily justified economically in view of the advantages of the remote reference technique. First, apart from data rejected in a preliminary screening, we were able to use all of the data collected to make reliable estimates of the apparent resistivities, even when the coherencies were as low as 0.1. Second, the simultaneous operation of the magnetotelluric stations obviously doubles the surveying rate compared with a single station. Thus, the remote reference technique may substantially reduce the time necessary to survey a given area.

## ACKNOWLEDGMENTS

We are grateful to Mr. Melendy and Mr. DeRosa for granting us access to their land. We are indebted to Professor H. F. Morrison and his students for the loan of equipment and for invaluable assistance. Professor Morrison and Dr. K. Vozoff kindly made helpful comments on the manuscript. This work was supported by the Divisions of Basic Energy Sciences and of Geothermal Energy, U.S. Department of Energy, and by the U.S.G.S. under grant number 14-08-0001-G-328.

REFERENCES

Clarke, J., Goubau, W. M., and Ketchen, M. B., 1976, Tunnel junction dc SQUID: fabrication, operation, and performance: J. Low Temp. Phys., v. 25, p. 99-144.

Goubau, W. M., Gamble, T. D., and Clarke, J., 1978, Magnetotelluric data analysis: removal of bias: submitted to Geophys.

Kao, D. W., and Rankin, D., 1977, Enhancement of signal to noise ratio in magnetotelluric data: Geophys., v. 42, p. 103-110.

Mazzella, A. T., 1965, Deep resistivity study across the San Andreas fault zone: Ph.D. thesis, University of California, Berkeley.

Morrison, H. F., Corwin, R. F., and Chang, M., 1977, High accuracy determination of temporal variations of crustal resistivity, J. G. Heacock, Ed., AGU Monograph 20. The Nature and Physical Properties of the Earth's Crust.

Sims, W. E., Bostick, F. X., Jr., and Smith, H. W., 1971, The estimation of magnetotelluric impedance tensor elements from measured data: Geophys., v. 36, p. 938-942.

Vozoff, K., 1972, The magnetotelluric method in the exploration of sedimentary basins: Geophys., v. 37, p. 98-41.

Table 1. Summary of filter bands, recording time per band, digitizer sampling period, and the number of points per fast Fourier transform (FFT).

| Filter band no. | Filter band (s) | Total recording time (h) | Digitizer sampling periods (s) | No. of points in data segments |
|---|---|---|---|---|
| 1 | 0.02 - 1 | 0.54 | 0.005 | 1024 |
| 2 | 0.33 - 5 | 4.22 | 0.1 | 512 |
| 3 | 3 - 100 | 10.52 | 1 | 512 |
| 4 | 30 - 100 | 14.9 | 10 | 256 |

Table 2. Number of harmonics per window, and numbers of sets of data segments for each station.

| Band no. 1 | | Band no. 2 | | Band no. 3 | | Band no. 4 | |
|---|---|---|---|---|---|---|---|
| Period (s) | Harmonics per window | Period (s) | Harmonics per window | Period (s) | Harmonics per window | Period (s) | Harmonics per window |
| 0.023 | 75 | 0.325 | 52 | 3.3 | 52 | 32.0 | 13 |
| 0.032 | 53 | 0.45 | 37 | 4.5 | 37 | 41.1 | 9 |
| 0.044 | 38 | 0.63 | 27 | 6.3 | 27 | 60.9 | 7 |
| 0.062 | 27 | 0.88 | 19 | 8.8 | 19 | 85.3 | 5 |
| 0.085 | 19 | 1.2 | 14 | 12 | 14 | | |
| 0.12 | 14 | 1.7 | 10 | 17 | 10 | | |
| 0.16 | 10 | 2.4 | 7 | 24 | 7 | | |
| 0.22 | 7 | 3.4 | 5 | 34 | 5 | | |
| 0.30 | 5 | | | 49 | 4 | | |
| 0.41 | 4 | | | | | | |
| 0.57 | 3 | | | | | | |
| 0.79 | 2 | | | | | | |

| | Number of sets of data segments | | | |
|---|---|---|---|---|
| Upper La Gloria | 476 | 297 | 73 | 21 |
| Lower La Gloria | 381 | 297 | 73 | 21 |

Table 3. Percent disagreement in apparent resistivities between bands.

| Bands | Remote reference | Standard | No. of values compared |
|---|---|---|---|
| 1,2 | 1.8 | 5.9 | 12 |
| 2,3 | 4.5 | 41.5 | 4 |
| 3,4 | 6.3 | 11.5 | 8 |

Table 4. Arrangement of data from bands 1 and 2 into blocks to estimate the standard deviation of the apparent resistivity at each period. Date refers to September 1977.

| Band 1 | | | | Band 2 | | | |
|---|---|---|---|---|---|---|---|
| | | Data block | | | | Data block | |
| Recording time | Date | Upper La Gloria | Lower La Gloria | Recording time | Date | Upper La Gloria | Lower La Gloria |
| 11:55 AM - 12:00 PM | 14 | 2 | Omitted | 9:25 AM - 9:50 AM | 14 | 1 | 1 |
| 12:01 PM - 12:06 PM | 14 | 3 | Omitted | 9:55 AM - 10:42 AM | 14 | 2 | 2 |
| 7:30 PM - 7:35 PM | 14 | 4 | 3 | 10:43 AM - 11:27 AM | 14 | 3 | 3 |
| 7:36 PM - 7:41 PM | 14 | 5 | 4 | 6:20 PM - 6:57 PM | 14 | 4 | 4 |
| 1:20 PM - 1:25 PM | 15 | 1 | 1 | 7:00 PM - 7:32 PM | 14 | 2 | 2 |
| 1:25 PM - 1:30 PM | 15 | 2 | 2 | 10:50 AM - 11:37 AM | 15 | 1 | 1 |
| 1:30 PM - 1:35 PM | 15 | 3 | 3 | 11:38 AM - 12:25 PM | 15 | 3 | 3 |
| 1:35 PM - 1:40 PM | 15 | 4 | 4 | 12:36 PM - 1:13 PM | 15 | 4 | 4 |
| 1:40 PM - 1:45 PM | 15 | 5 | 1 | | | | |
| 1:45 PM - 1:50 PM | 15 | 1 | 2 | | | | |

Table 5. Expected standard deviations, $100\ \sigma_j/\bar{\rho}_j$, of mean apparent resistivities from the remote reference method.

| Period (s) | Upper La Gloria | | Lower La Gloria | |
|---|---|---|---|---|
| | $100\ \sigma_{xy}/\bar{\rho}_{xy}$ | $100\ \sigma_{yx}/\bar{\rho}_{yx}$ | $100\ \sigma_{xy}/\bar{\rho}_{xy}$ | $100\ \sigma_{yx}/\bar{\rho}_{yx}$ |
| 0.03 | 0.4 | 3.5 | 2.0 | 2.3 |
| 0.04 | 0.5 | 0.8 | 0.7 | 0.8 |
| 0.06 | 0.2 | 0.8 | 1.3 | 0.5 |
| 0.08 | 0.3 | 2.1 | 1.1 | 0.9 |
| 0.12 | 0.5 | 0.7 | 0.8 | 0.7 |
| 0.16 | 0.4 | 1.4 | 1.6 | 1.3 |
| 0.22 | 0.7 | 0.6 | 1.9 | 1.1 |
| 0.30 | 0,6 | 0.9 | 0.9 | 1.8 |
| 0.41 | 0,04 | 4.4 | 0.7 | 1.2 |
| 0.57 | 1.2 | 2.2 | 1.3 | 1.3 |
| 0.79 | 1.2 | 1.6 | 1.8 | 1.5 |
| 0.33 | 2.2 | 1.6 | 0.4 | 0.8 |
| 0.45 | 0.8 | 1.0 | 1.2 | 0.5 |
| 0.63 | 1.2 | 3.0 | 1.0 | 0.5 |
| 0.88 | 1.2 | 0.9 | 0.9 | 0.7 |
| 1.2 | 1.0 | 1.3 | 1.4 | 1.1 |
| 1.7 | 1.1 | 1.4 | 0.9 | 1.5 |
| 2.4 | 0.8 | 3.4 | 2.7 | 1.2 |
| 3.4 | 1.3 | 2.6 | 1.7 | 2.0 |

FIGURE CAPTIONS

Fig. 1. Magnetotelluric measurement sites in Bear Valley, California. ◎ magnetometer; ● electrode.

Fig. 2. Block diagram of data acquisition.

Fig. 3. Standard method apparent resistivities vs. period, Upper La Gloria. --- remote reference results.

Fig. 4. Admittance method apparent resistivities vs. period, Upper La Gloria. --- remote reference results.

Fig. 5. Crosspower method apparent resistivities vs. period, Upper La Gloria. --- remote reference results.

Fig. 6. Remote reference method apparent resistivities vs. period, Upper La Gloria.

Fig. 7. Coherency between the measured electric field and the electric field predicted by the standard method of analysis, Upper La Gloria.

Fig. 8. Orientation angle $\theta_x$ between rotated x-axis and magnetic north, skewness, and phase anglesvs. period, standard method, Upper La Gloria.

Fig. 9. Orientation angle $\theta_x$ between rotated x-axis and magnetic north, skewness, and phase angles vs. period, remote reference method, Upper La Gloria.

Fig. 10. Standard method apparent resistivities vs. period, Lower La Gloria. --- remote reference results.

Fig. 11. Admittance method apparent resistivities vs. period, Lower La Gloria. --- remote reference results.

Fig. 12. Crosspower method apparent resistivities vs. period, Lower La Gloria. --- remote reference results.

Fig. 13. Remote reference method apparent resistivities vs. period, Lower La Gloria.

Fig. 14. Coherency between the measured electric field and the electric field predicted by the standard method of analysis, Lower La Gloria.

Fig. 15. Orientation angle $\theta_x$ between rotated x-axis and magnetic north, skewness, and phase angles vs. period, standard method, Lower La Gloria.

Fig. 16. Orientation angle $\theta_x$ between rotated x-axis and magnetic north, skewness, and phase angles vs. period, remote reference method, Lower La Gloria.

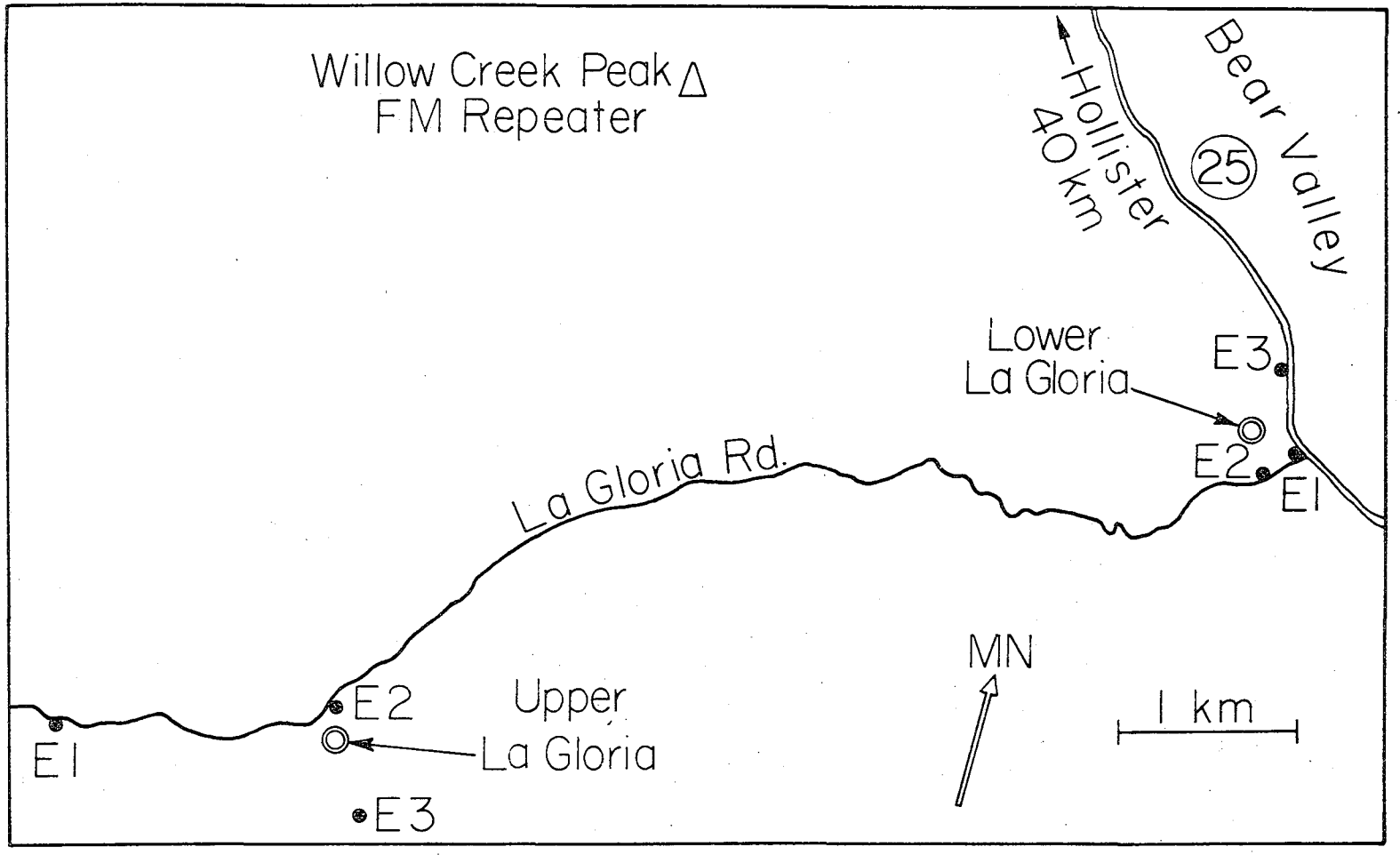


XBL7712-6514

Fig. 1

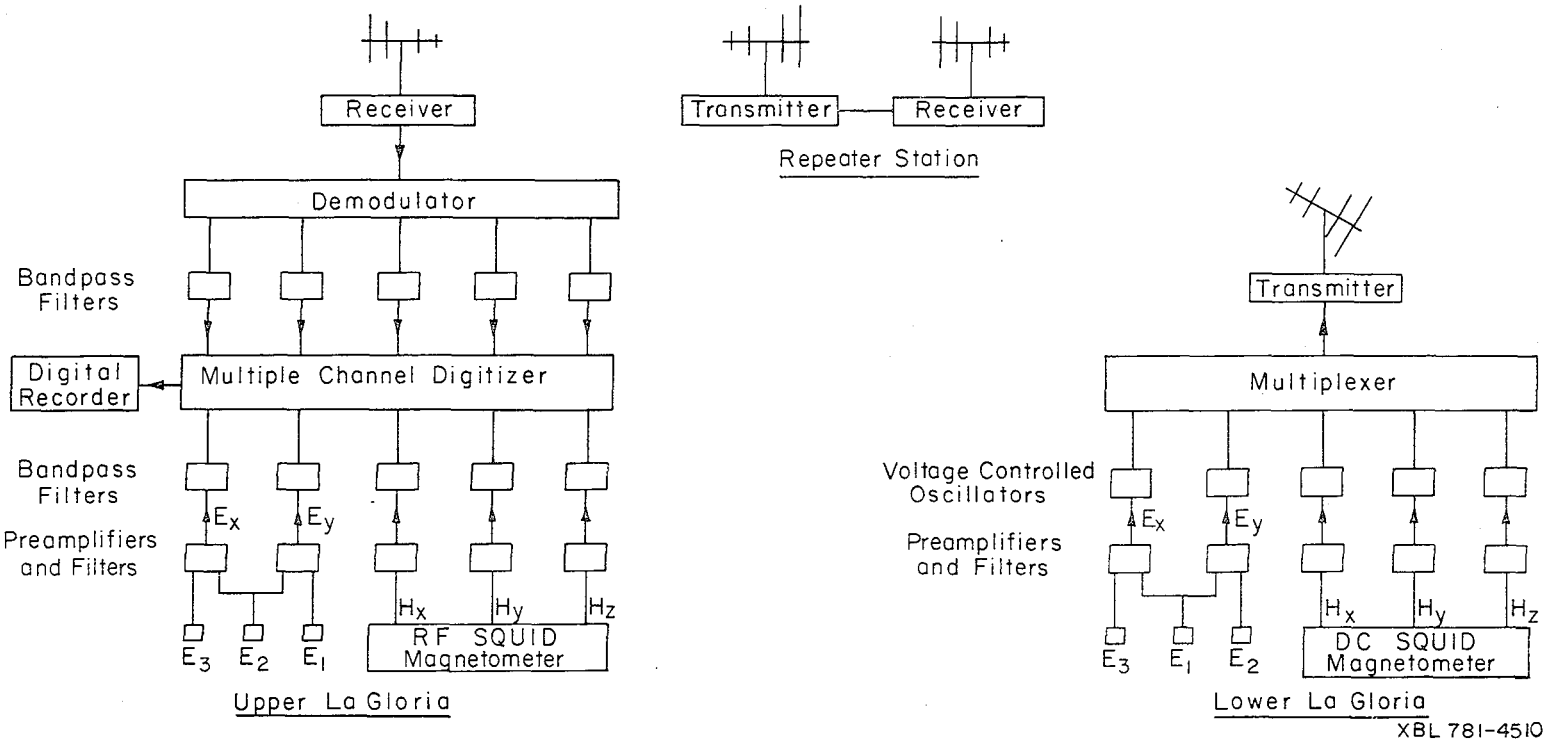
Receiver
Demodulator
Bandpass Filters
Digital Recorder
Multiple Channel Digitizer
Bandpass Filters
Preamplifiers and Filters
Ex
Ey
Hx
Hy
Hz
E3
E2
E1
RF SQUID Magnetometer
Upper La Gloria
Transmitter
Receiver
Repeater Station
Transmitter
Multiplexer
Voltage Controlled Oscillators
Preamplifiers and Filters
Ex
Ey
Hx
Hy
Hz
E3
E1
E2
DC SQUID Magnetometer
Lower La Gloria
XBL 781-4510

Fig. 2

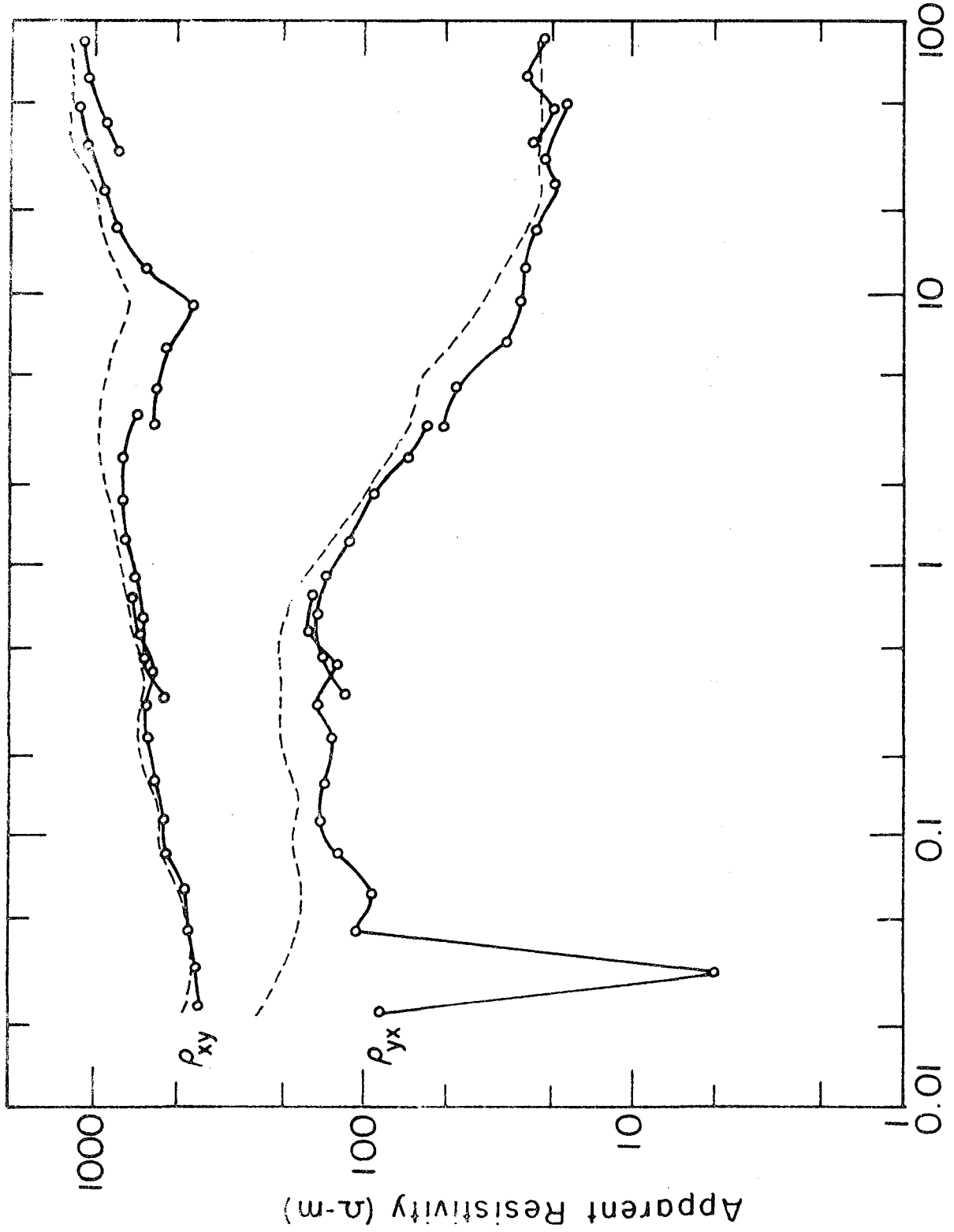
Apparent Resistivity (Ω-m)
1000
100
10
1
0.01
0.1
1
10
100
Period (s)
$\rho_{xy}$
$\rho_{yx}$
XBL 7712-6513

Fig. 3

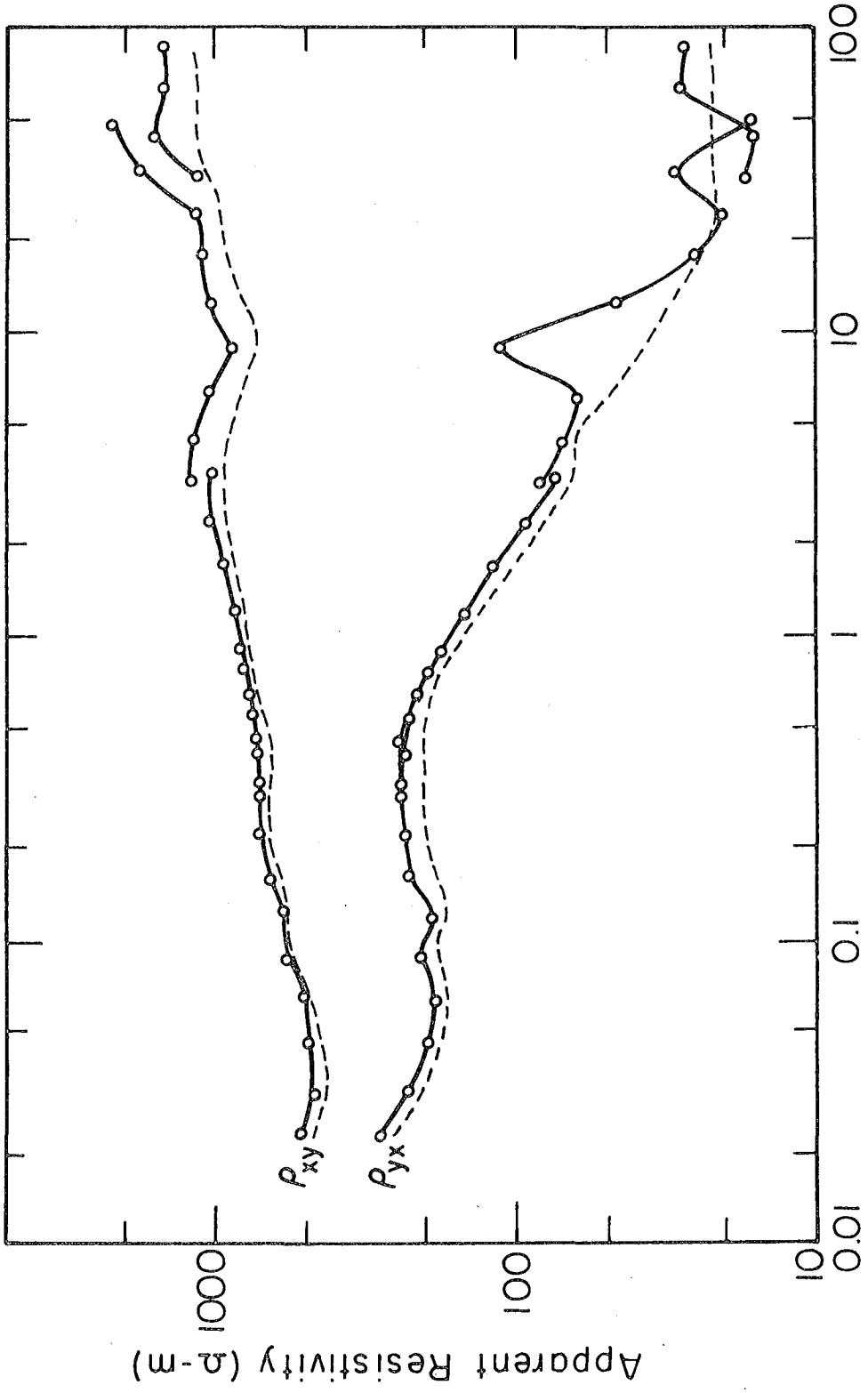


XBL 7712-6517

Fig. 4

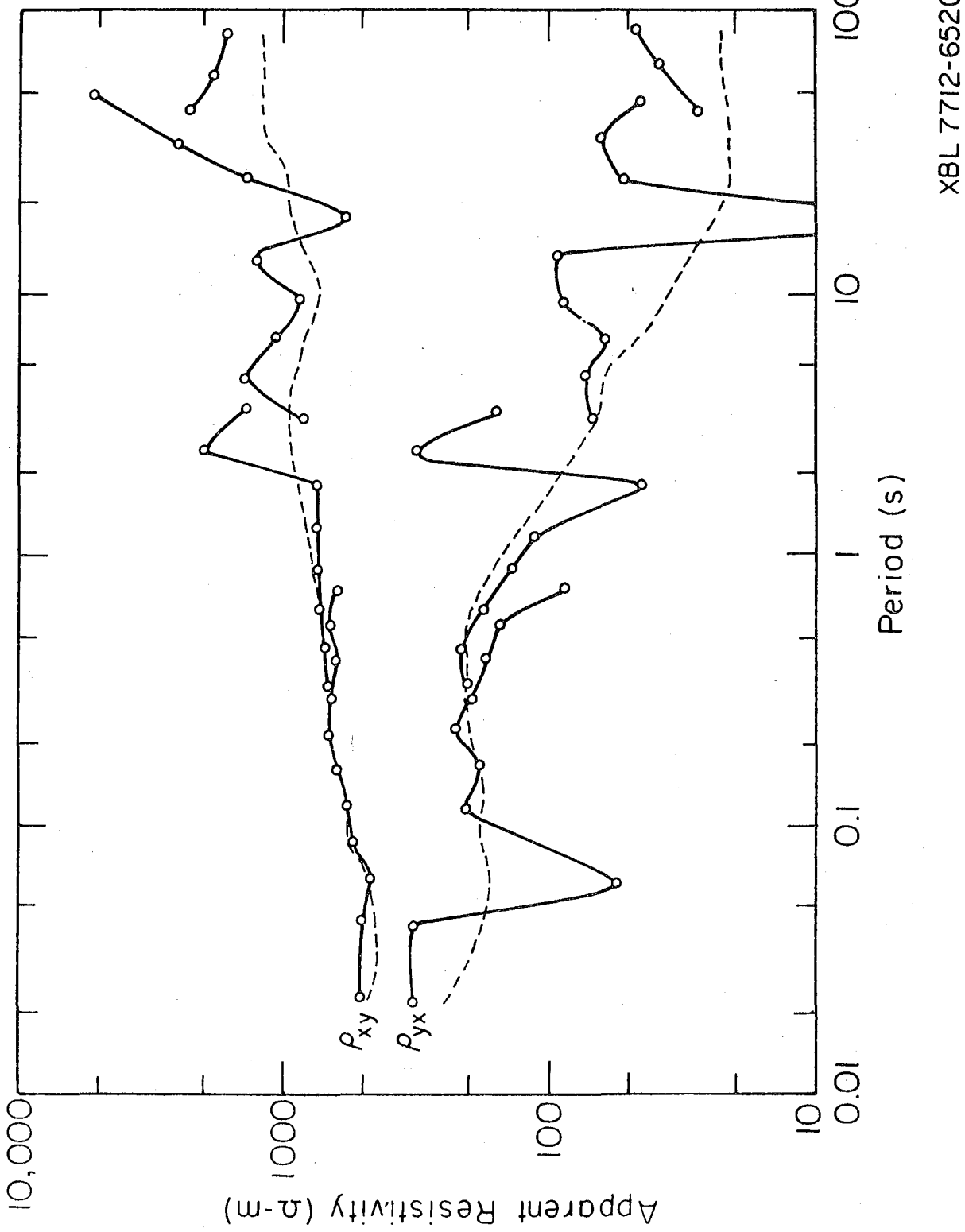
Apparent Resistivity (Ω-m)
10,000
1000
100
10
0.01
0.1
1
10
100
Period (s)
$\rho_{xy}$
$\rho_{yx}$
XBL 7712-6520

Fig. 5

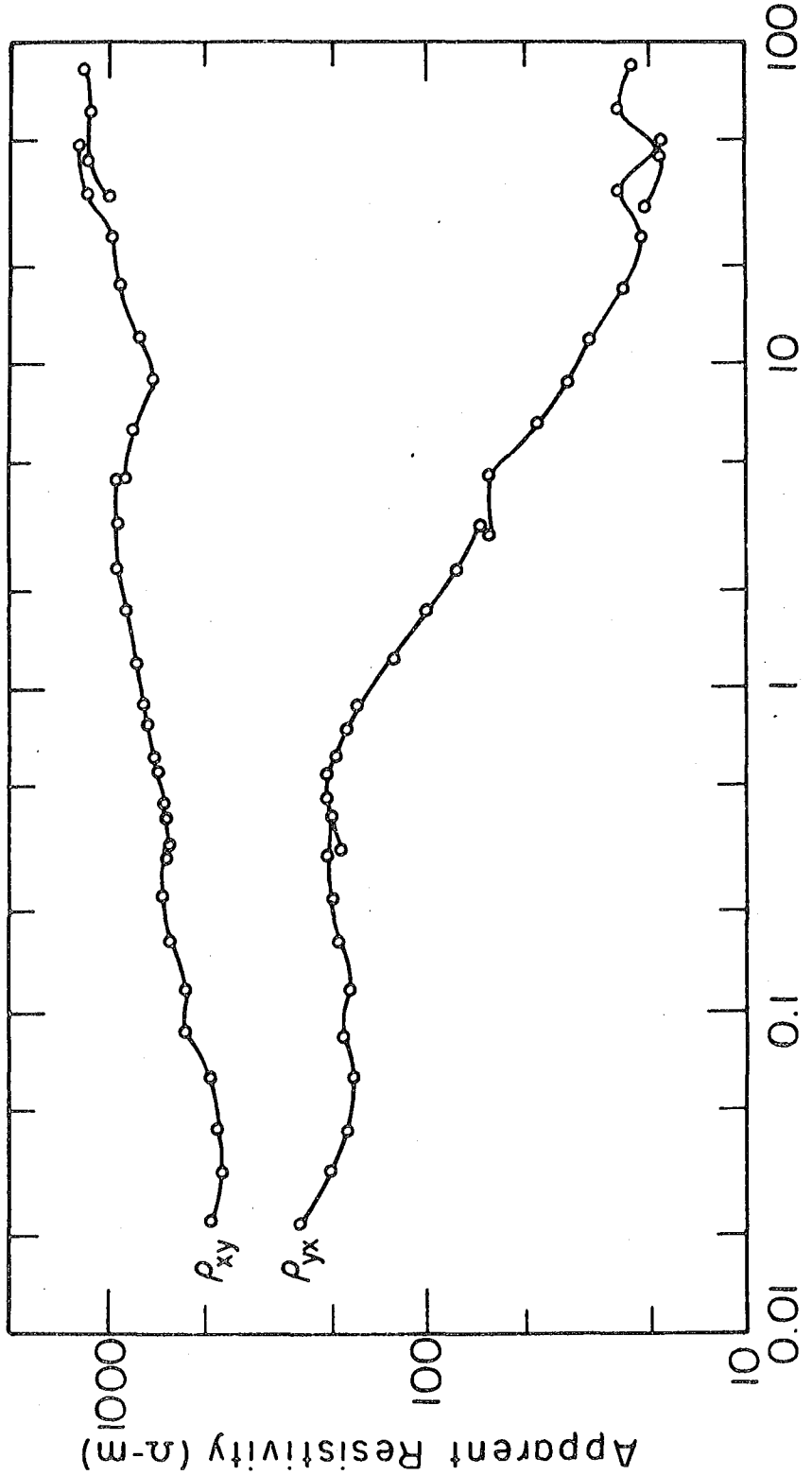
Apparent Resistivity (Ω-m)
1000
100
10
0.01
0.1
1
10
100
Period (s)
$\rho_{xy}$
$\rho_{yx}$
XBL 7712-6511

Fig. 6

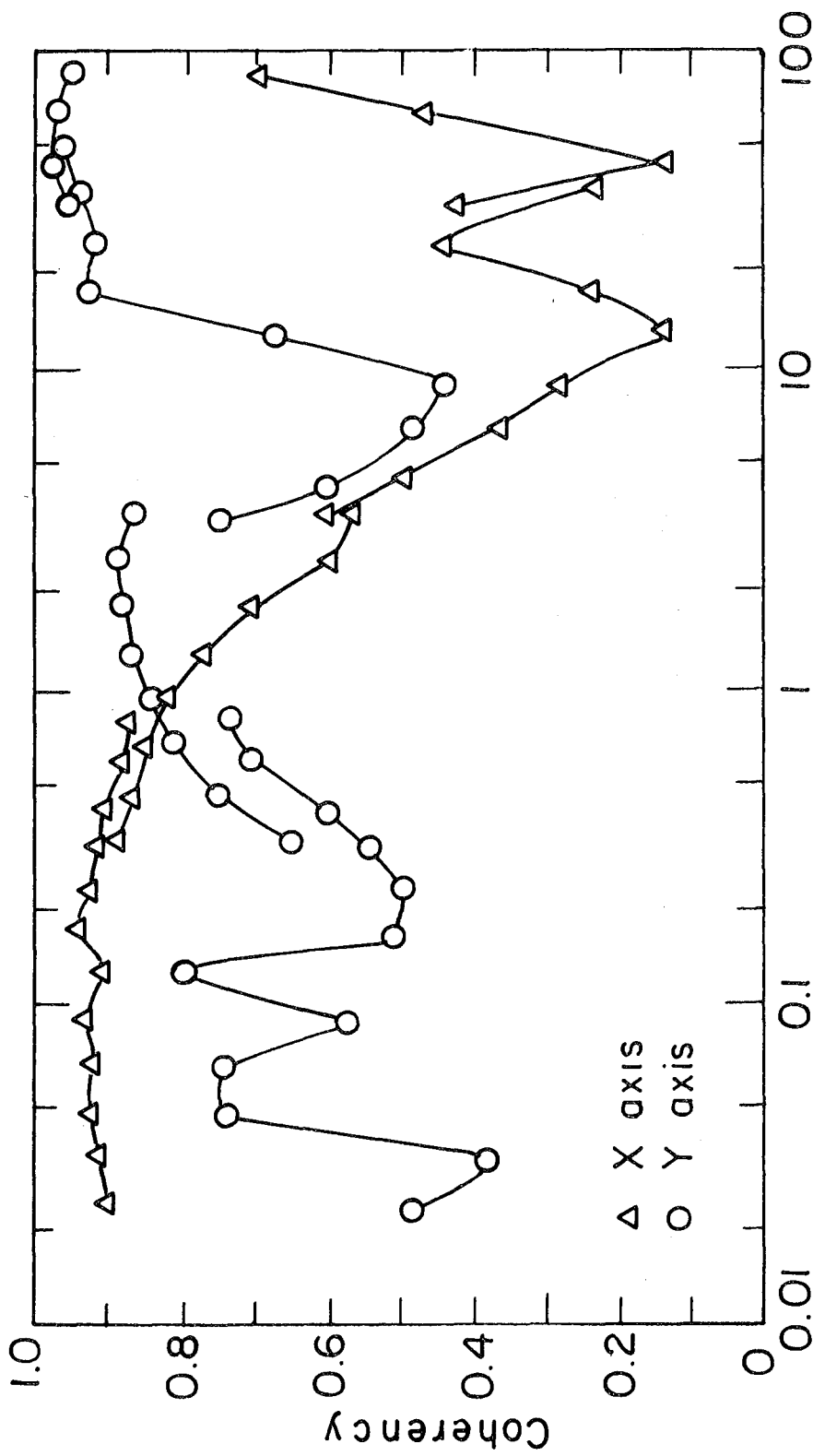


XBL 7712-6515

Fig. 7

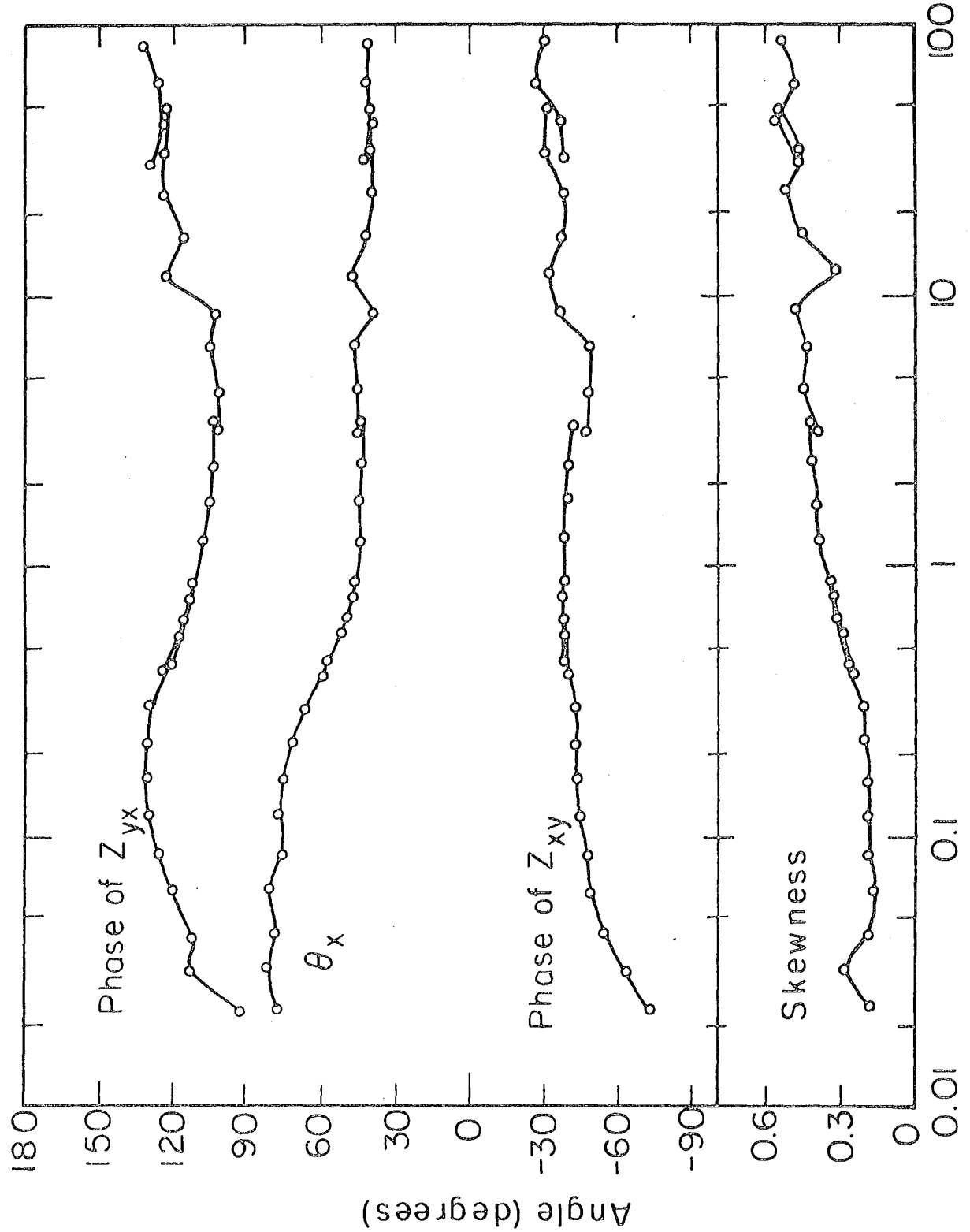


XBL 7712-6523

Fig. 8

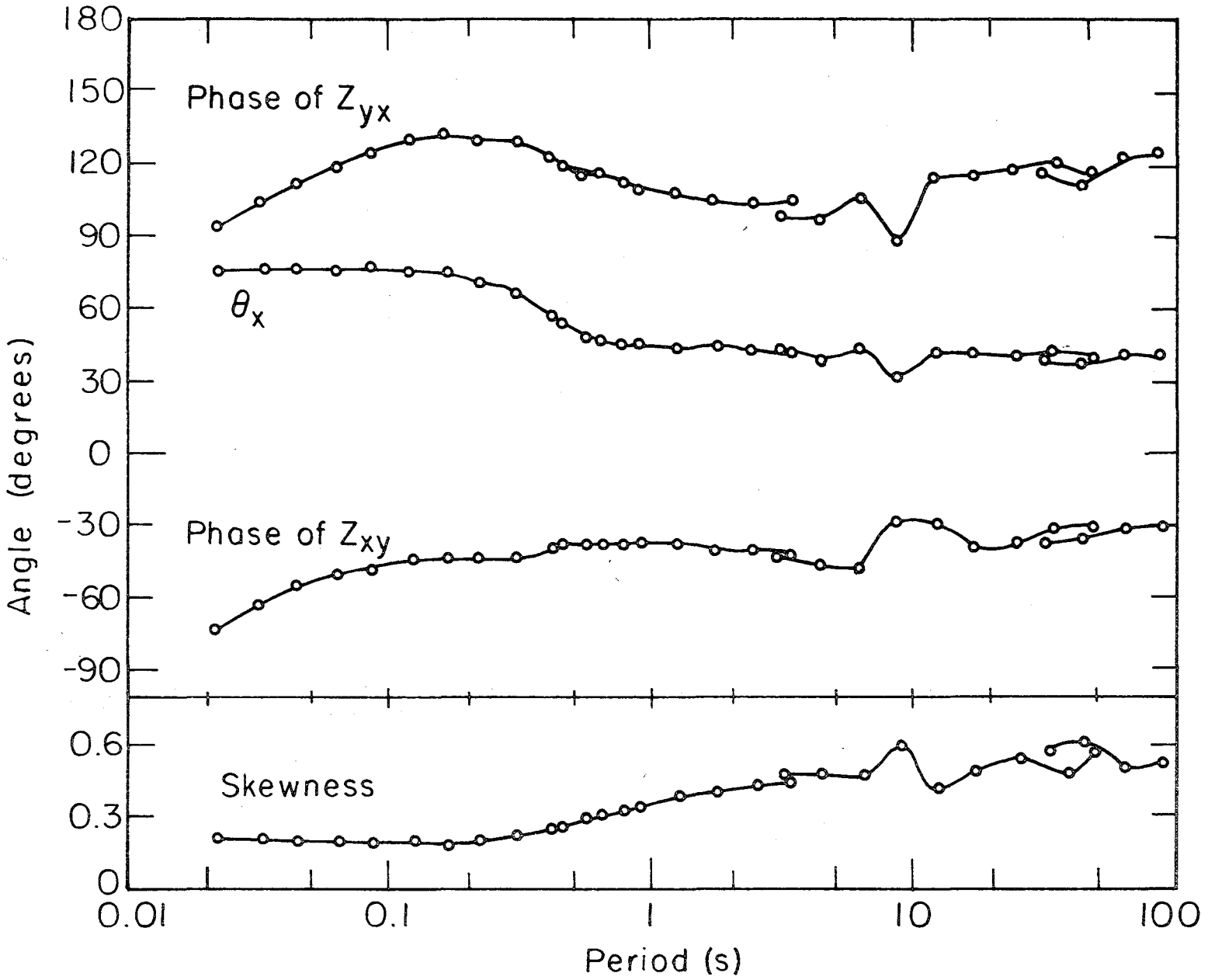
180
150
120
90
60
30
0
-30
-60
-90
Angle (degrees)
Phase of $Z_{yx}$
$\theta_x$
Phase of $Z_{xy}$
0.6
0.3
0
Skewness
0.01
0.1
1
10
100
Period (s)
XBL7712-6522

Fig. 9

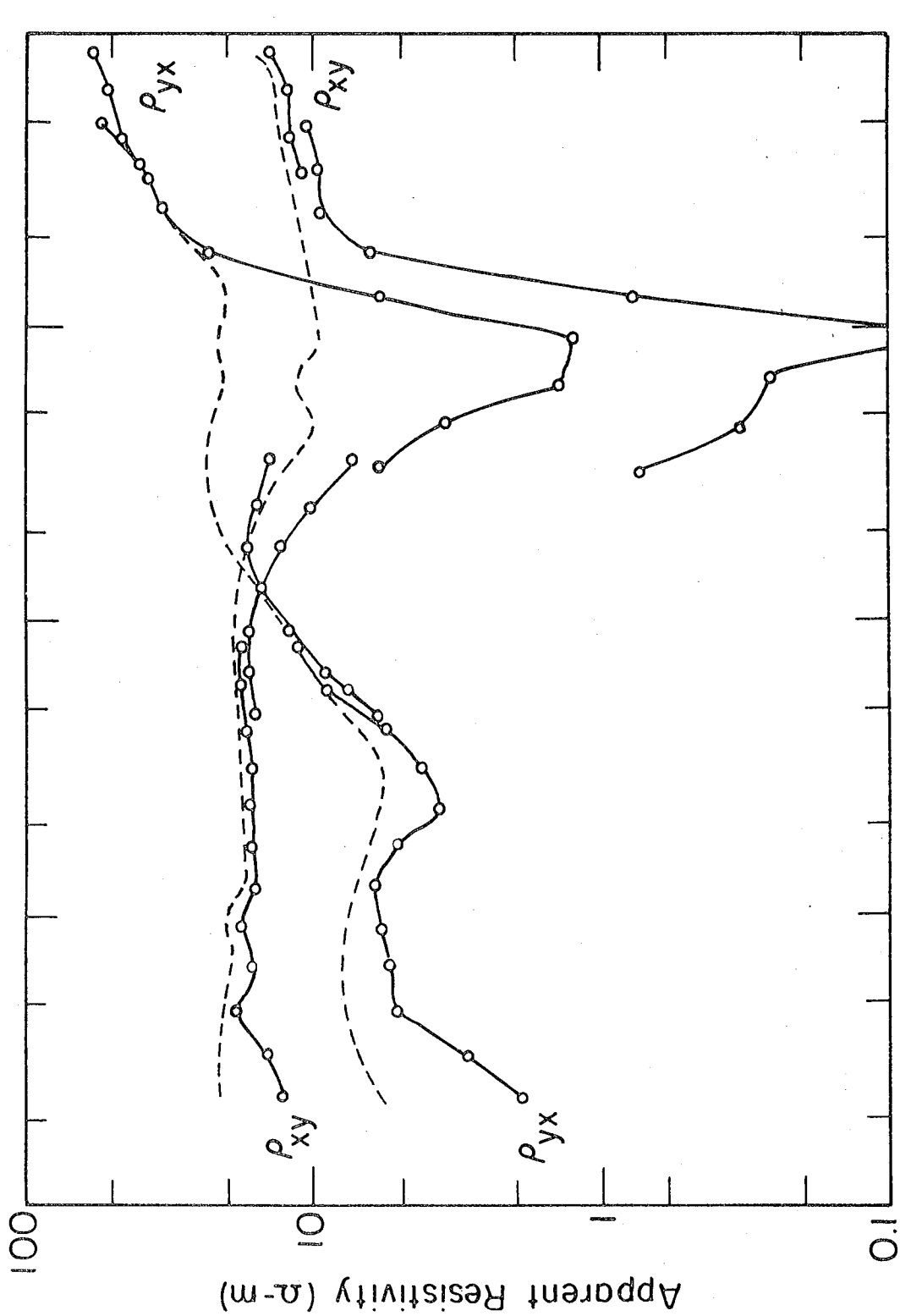


XBL 7712-6512

Fig. 10

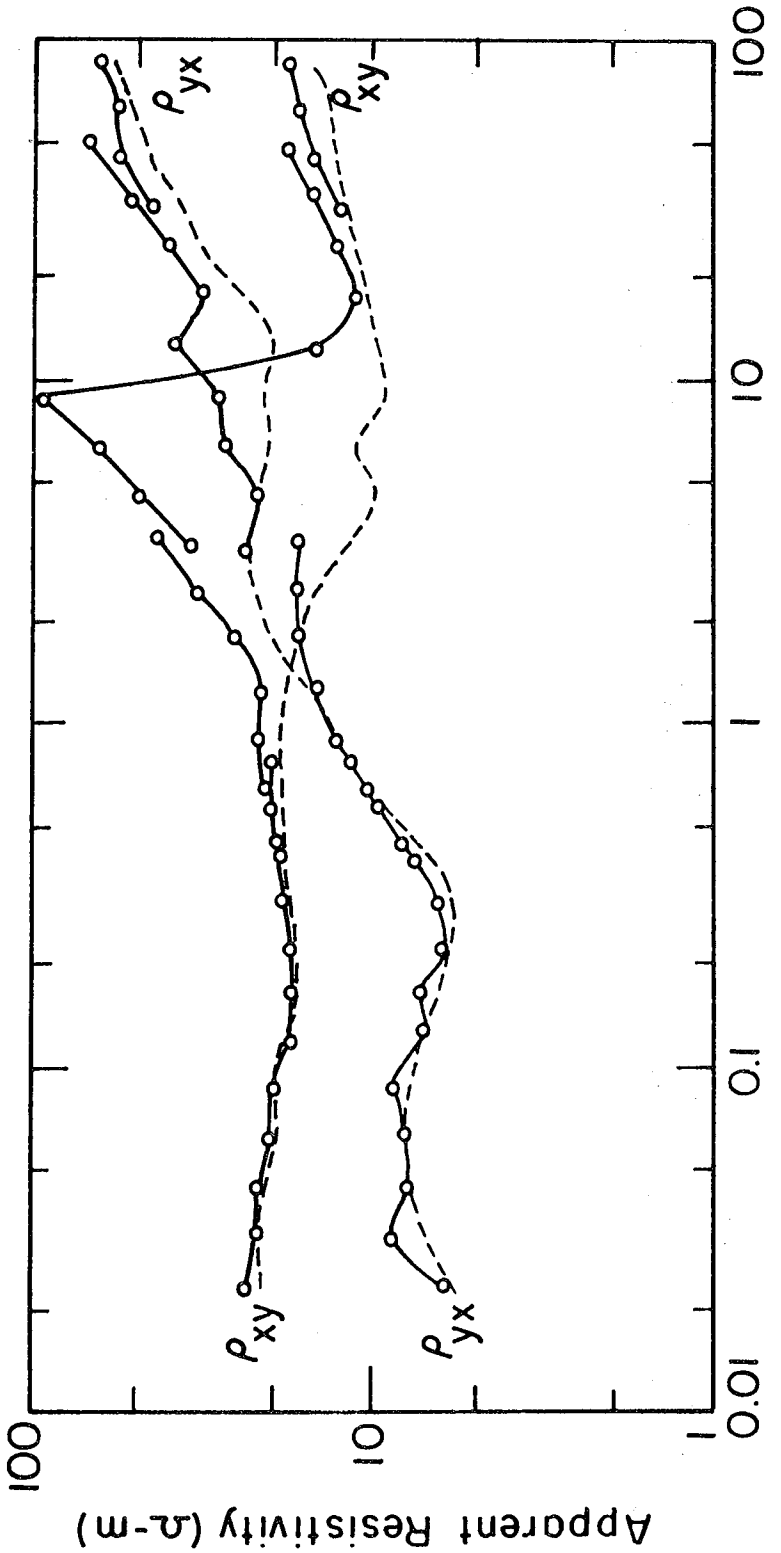


XBL 7712-6518

Fig. 11

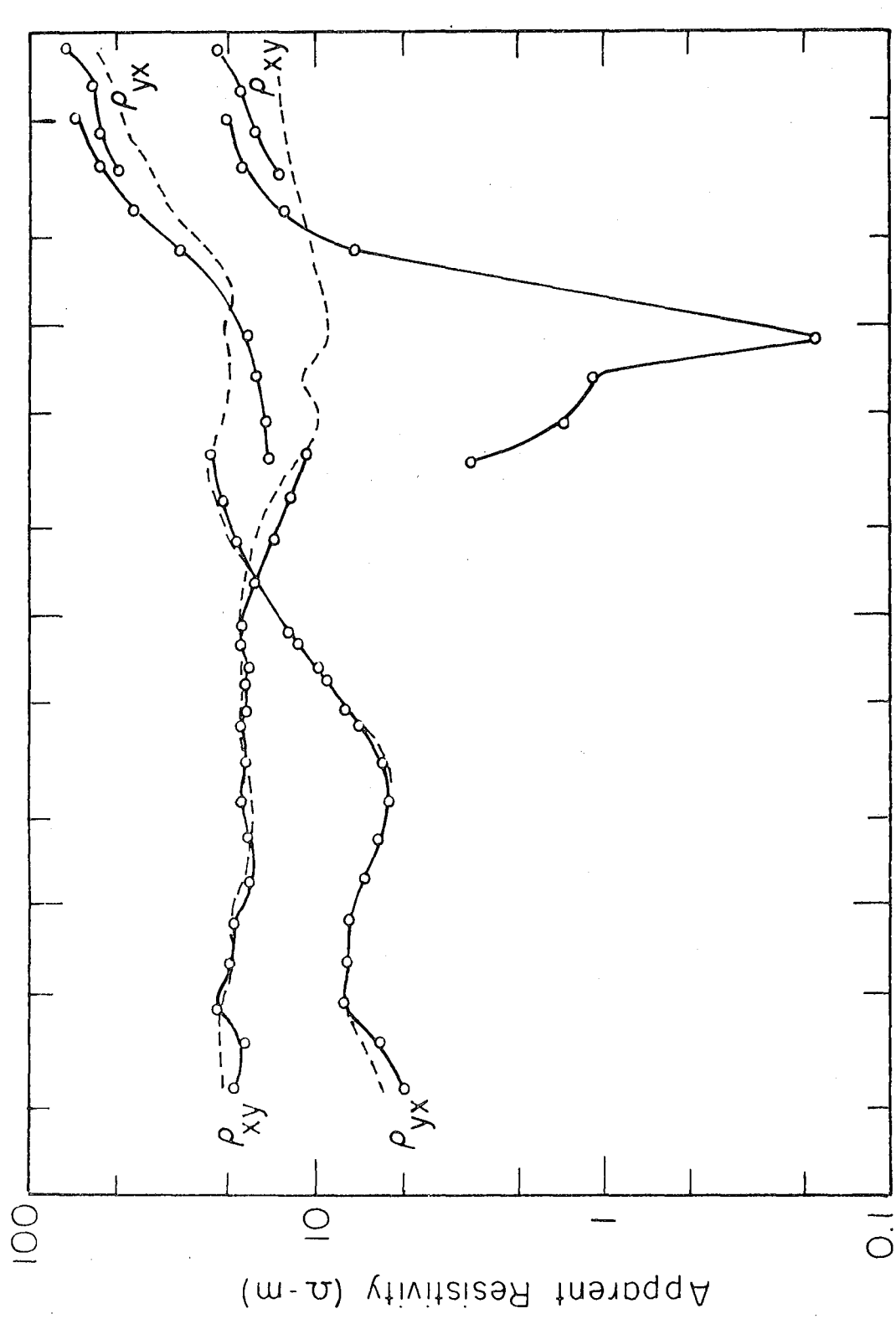


XBL 7712-6519

Fig. 12

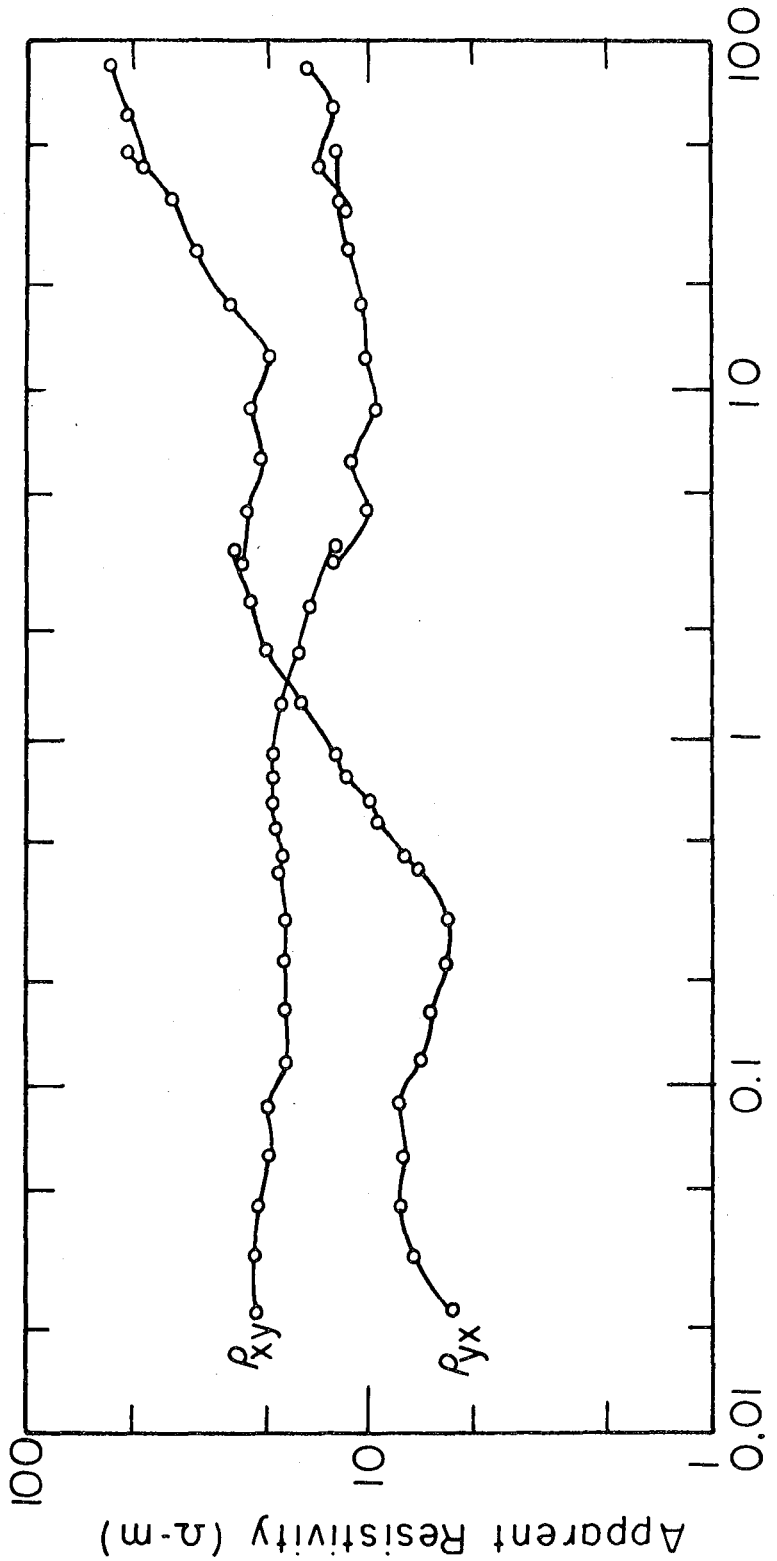
Apparent Resistivity (Ω-m)
100
10
1
0.01
0.1
1
10
100
Period (s)
$\rho_{xy}$
$\rho_{yx}$
XBL 7712-6510

Fig. 13

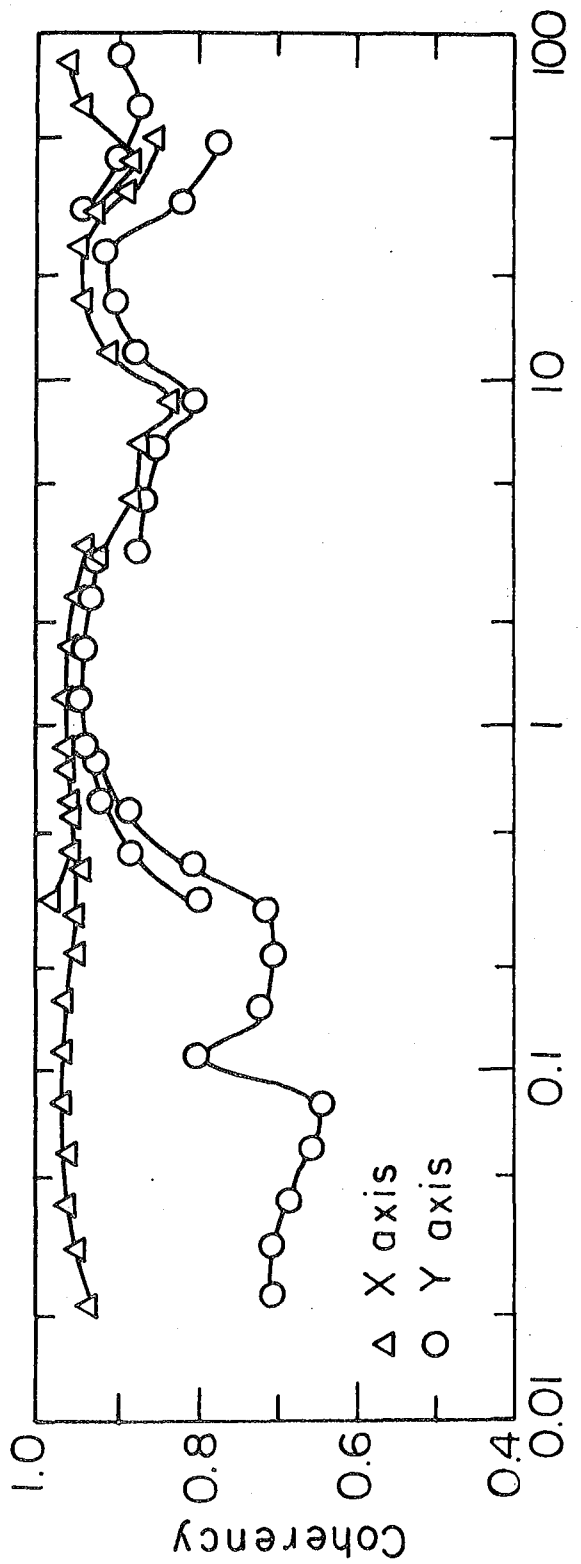


XBL 7712-6516

Fig. 14

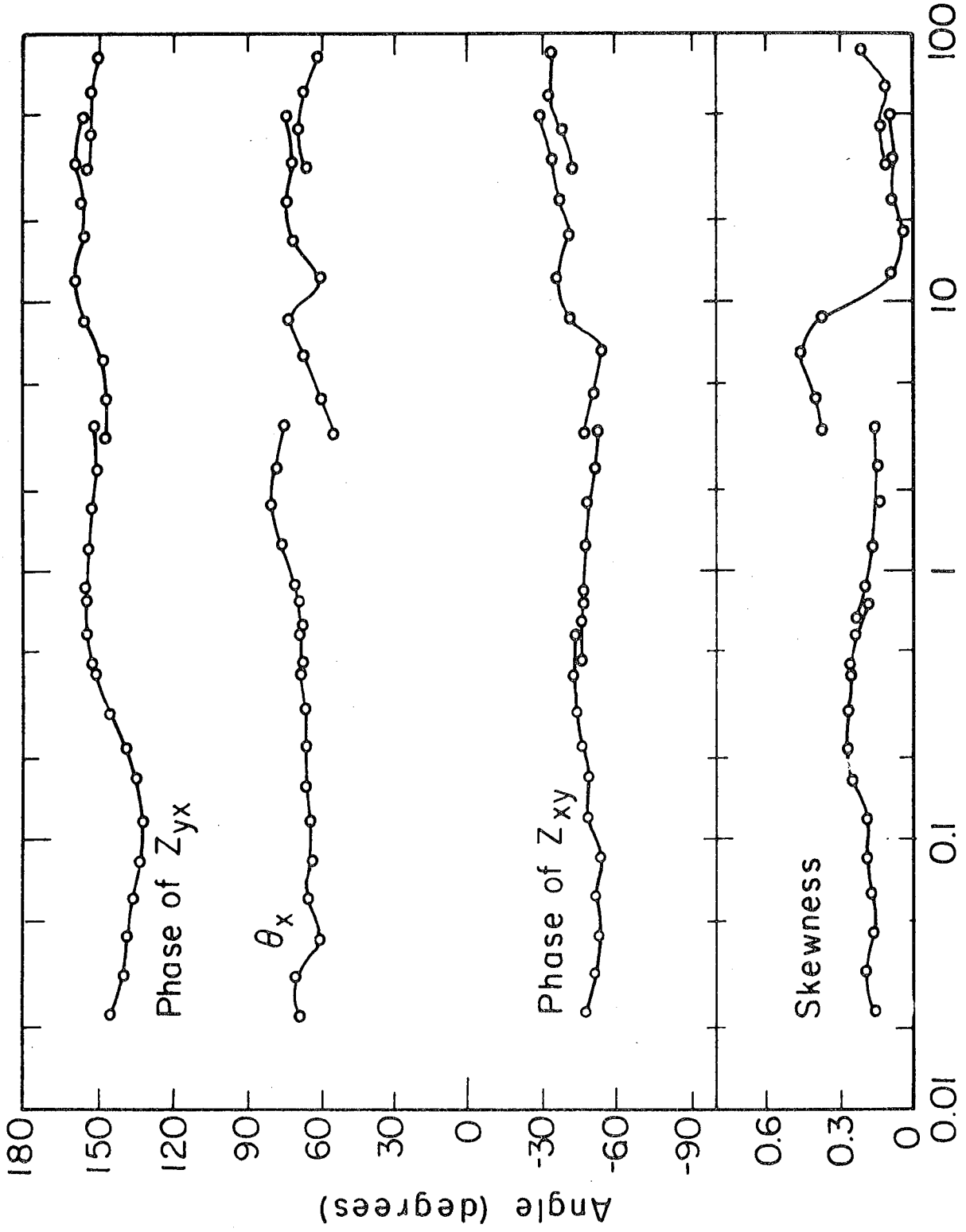


XBL7712-6524

Fig. 15

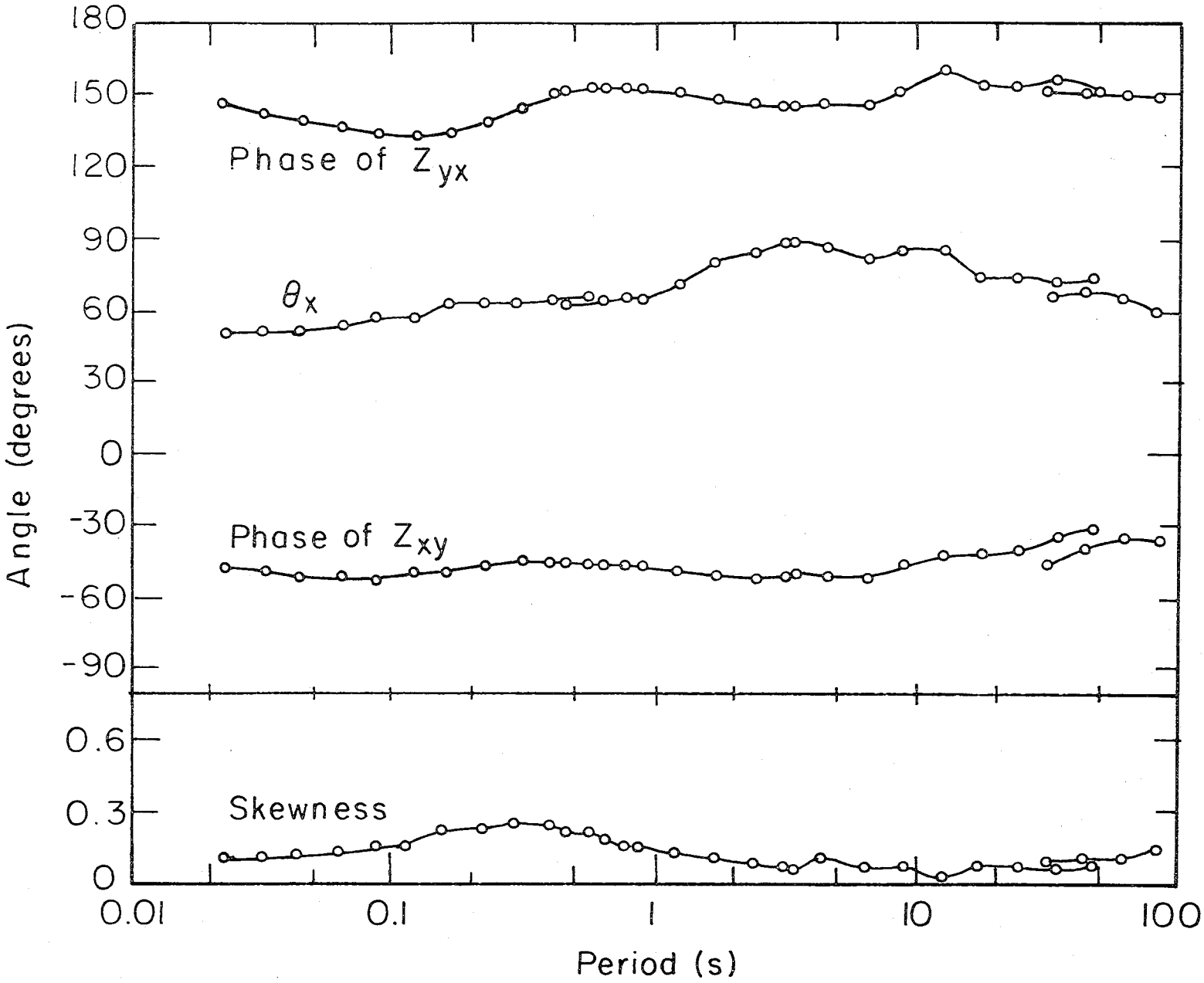


XBL 7712-6521

Fig. 16

This report was done with support from the United States Energy Research and Development Administration. Any conclusions or opinions expressed in this report represent solely those of the author(s) and not necessarily those of The Regents of the University of California, the Lawrence Berkeley Laboratory or the United States Energy Research and Development Administration.